Advanced Composite Materials
Publication details, including instructions for authors and subscription information:
http://www.tandfonline.com/loi/tacm20

Real-Time Monitoring of Composite Wind Turbine Blades Using Fiber Bragg Grating Sensors

Sunho Park [a], Taesung Park [b] & Kyungseop Han [c]

[a] Department of Mechanical Engineering, Pohang University of Science and Technology, San 31, Hyoja-dong, Nam-gu, Pohang, Gyungbuk 790-784, Korea

[b] Department of Mechanical Engineering, Pohang University of Science and Technology, San 31, Hyoja-dong, Nam-gu, Pohang, Gyungbuk 790-784, Korea

[c] Department of Mechanical Engineering, Pohang University of Science and Technology, San 31, Hyoja-dong, Nam-gu, Pohang, Gyungbuk 790-784, Korea

Version of record first published: 02 Apr 2012.

To cite this article: Sunho Park , Taesung Park & Kyungseop Han (2011): Real-Time Monitoring of Composite Wind Turbine Blades Using Fiber Bragg Grating Sensors, Advanced Composite Materials, 20:1, 39-51

To link to this article: http://dx.doi.org/10.1163/092430410X504198

VSP

Advanced Composite Materials 20 (2011) 39–51

ADVANCED COMPOSITE MATERIALS
brill.nl/acm

Real-Time Monitoring of Composite Wind Turbine Blades Using Fiber Bragg Grating Sensors

Sunho Park, Taesung Park and Kyungseop Han *

Department of Mechanical Engineering, Pohang University of Science and Technology, San 31, Hyoja-dong, Nam-gu, Pohang, Gyungbuk 790-784, Korea

Received 8 September 2009; accepted 11 November 2009

Abstract

The prototype of a 2 MW wind turbine (type U88) has been tested at Taebaek, South Korea since January 2009. A real-time monitoring system with fiber Bragg grating (FBG) sensors was designed and applied to monitor wind turbine blades in operation. Differences according to the operating conditions (yawing, pitching and start-up/normal operation) were monitored accurately in real time with sensors. Additionally, using commercial FEM codes, a GFRP-based composite rotor blade was modeled, and then natural frequencies obtained from the FE modal analysis were compared with the FFT results of measured strain data. Finally, this paper provides an overview of the real-time monitoring system setups and some current test results including modal characteristics.

Keywords

Real-time monitoring, composite wind turbine blade, fiber Bragg grating (FBG) sensor, natural frequency, FE modal analysis

1. Introduction

In recent years, condition monitoring in wind turbine applications is becoming more and more common [1]. Rotor blades in particular require monitoring systems to reduce maintenance costs, to detect small problems before they become large defects, and to improve the operation time of the wind turbine. Fiber Bragg grating (FBG) sensing is an established technology for temperature and strain measurement. It provides electromagnetic interference immunity, multiplexed operation and strong compatibility with composites, which are the main materials of rotor blades. Because of these advantages, FBG sensors have been used for rotor blade monitoring [2, 3].

* To whom correspondence should be addressed. E-mail: kshan@postech.ac.kr
Edited by KSCM

 DOI:10.1163/092430410X504198

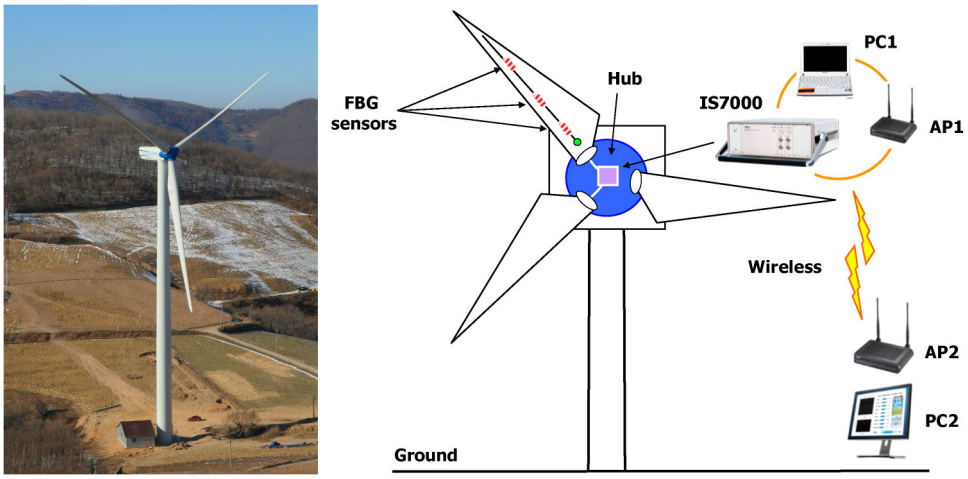

Figure 1. 2 MW wind turbine with a wireless network. This figure is published in color on http://www.ingentaconnect.com/content/vsp/acm

In our previous research [4], two FBG sensors were embedded in the 750 kW composite rotor blade skin, and full-scale structural tests were monitored. The sensors had an excellent resolution in the time domain and detected a frequency response up to 100 Hz, proving their reliability as a condition monitoring system. Also, GFRP-based composite rotor blades were simulated using commercial FEM codes to analyze their dynamic responses. Measurement and calculation of flapwise and chordwise natural frequencies were performed and compared. However, rotor blades with a length of more than 30 m also require determination of the 2nd natural frequency in the flapwise direction [8].

In this paper, a real-time FBG monitoring system was designed and applied to monitor the 42.65 m long rotor blade of a 2 MW wind turbine (type U88, see Fig. 1) at Taebaek, South Korea. Under various operating conditions, the wind turbine performance is analyzed.

2. Experimental

2.1. Monitoring System

The 2 MW wind turbine with the wireless network of two access points (AP1 and AP2) is shown in Fig. 1. Also, the real-time FBG monitoring system and its steel bracket on the hub are shown in Fig. 2. IS7000 (Fiberpro Inc.) is a commercial FBG interrogator with WDM (wavelength–division–multiplexing) techniques. It has a modular structure — main frame, laser module and sensor modules. Table 1 lists the specifications of the IS7000. The measurement results from IS7000 are processed, displayed and stored in a laptop computer (PC1) installed with driving software. PC1 is directly controlled using the remote control software, NQVM [5], on the

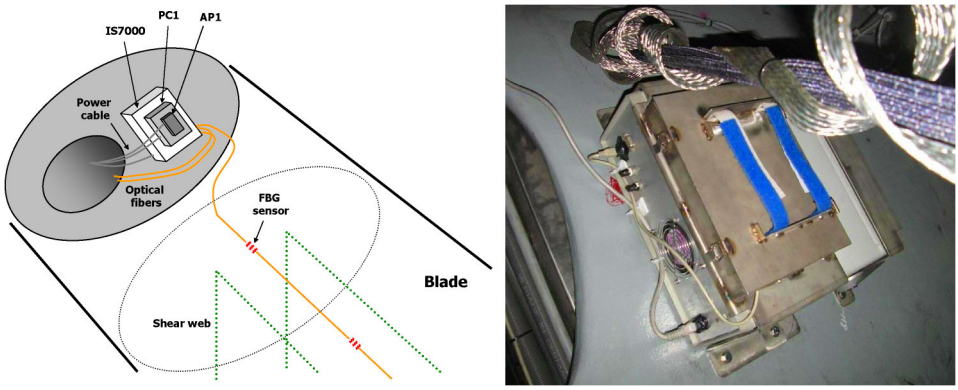

Figure 2. Real-time FBG monitoring system. This figure is published in color on http://www.ingentaconnect.com/content/vsp/acm

Table 1.
Specifications for IS7000

Laser module (wavelength swept laser):	
Wavelength range	35 nm (1530–1565 nm)
Sweep frequency	200 Hz
Sensor module:	
Wavelength repeatability	$<\pm 2$ pm
Wavelength accuracy	$<\pm 10$ pm
Wavelength resolution	1 pm
Sampling frequency (measurement speed)	200 Hz
Multi-channel capability	4 sensor channels
Others:	
Operating temperature	10–40°C
Dimensions	364 × 363 × 147 mm
Interface	USB
Optical connector	FC/APC
Driving software	LabView 6.0

ground computer (PC2). The power supply (220 V/60 Hz) is available in the rotating hub.

2.2. *FBG Sensors*

Basically, the FBG sensor is based on the measurement of the changes in a reflected signal, which is the center wavelength of back-reflected light from a Bragg grating, and depends on the effective refractive index of the core and the periodicity of the grating. According to the Bragg condition, the Bragg wavelength can be expressed as $\lambda_B = 2n_{\text{eff}}\Lambda$, where λ_B is the Bragg grating wavelength, Λ is the grating periodic spacing, and n_{eff} is the effective refractive index of the fiber core [6]. When an external mechanical or thermal deformation is imposed on the grating area, the effective

refractive index and the periodic spacing will be changed. The Bragg wavelength shift ($\Delta\lambda_B$) caused by the change of strain ($\Delta\varepsilon$) and change of temperature (ΔT) can be expressed as the following equations:

$$\Delta\lambda_B = \Delta\lambda_{B,\Delta\varepsilon} + \Delta\lambda_{B,\Delta T} \tag{1}$$

and

$$\Delta\lambda_{B,\Delta\varepsilon} = \lambda_B(1 - p_e)\Delta\varepsilon, \qquad \Delta\lambda_{B,\Delta T} = \lambda_B(\alpha - \xi)\Delta T, \tag{2}$$

where p_e is the fiber's effective photoelastic coefficient ($\sim$0.23), α is the thermal expansion coefficient for the fiber and ξ is the thermo-optic coefficient.

Figure 3(a) shows the blade sensor array layout. The acrylate coated FBG sensors (Avensys Inc.) have an outside diameter of 250 μm and a grating length of 14 mm. Temperature compensation sensors (1531 nm) are located at the root ($R = 1.2$ m)

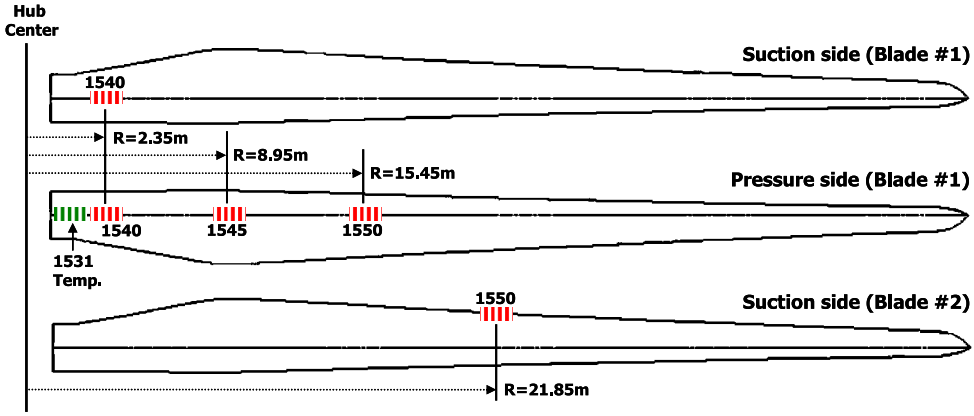

(a)

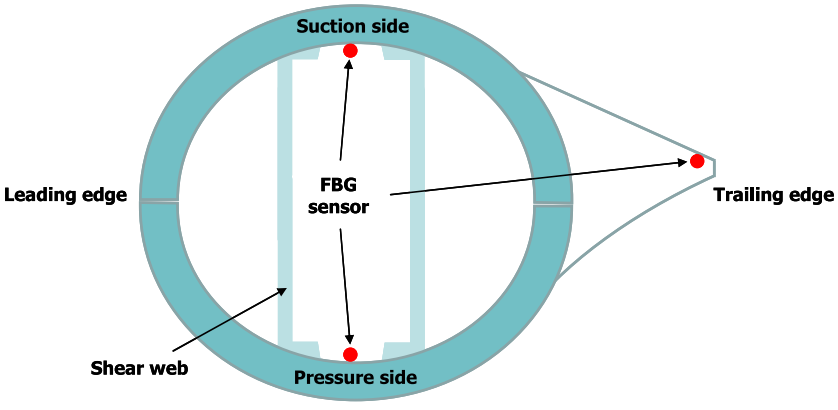

(b)

Figure 3. Scheme of the FBG sensor positions. This figure is published in color on http://www.ingentaconnect.com/content/vsp/acm

of Blade #1. Strain sensors are located 2.35 m, 8.95 m, 15.45 m and 21.85 m from the hub center. Here we used three Bragg wavelengths, 1540 nm, 1545 nm and 1550 nm. FBG sensors are located on the inside of the blade and mounted parallel to the neutral axis of the blade, except one near the trailing edge as shown in Fig. 3(b). Unidirectional E-glass tape was used to laminate FBG sensors onto the blade surface by the hand lay-up process.

3. Results and Discussion

3.1. Strain Measurements

Figure 4 shows the initial position of rotor blades at the beginning of the measurement. In this blade direction, the FBG monitoring system was set to zero. Reflected wavelengths were detected with a 100 Hz sampling rate. Figures 5 and 6 show strain time series calculated by substituting wavelengths reflected from FBG sensors into equations (1) and (2). These signals were compared with video of the wind turbine at the same time. At first, the rotor blades were completely out of the wind (90° pitch angle) under windless conditions. During seconds 1340 to 1400, the wind

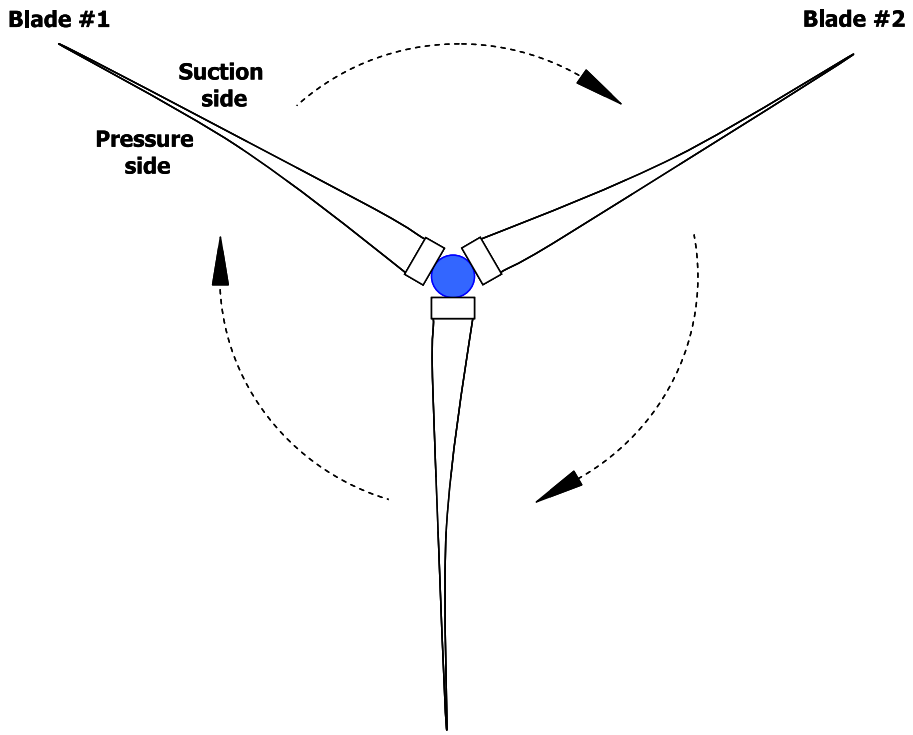

Figure 4. Initial position of rotor blades. This figure is published in color on http://www.ingentaconnect.com/content/vsp/acm

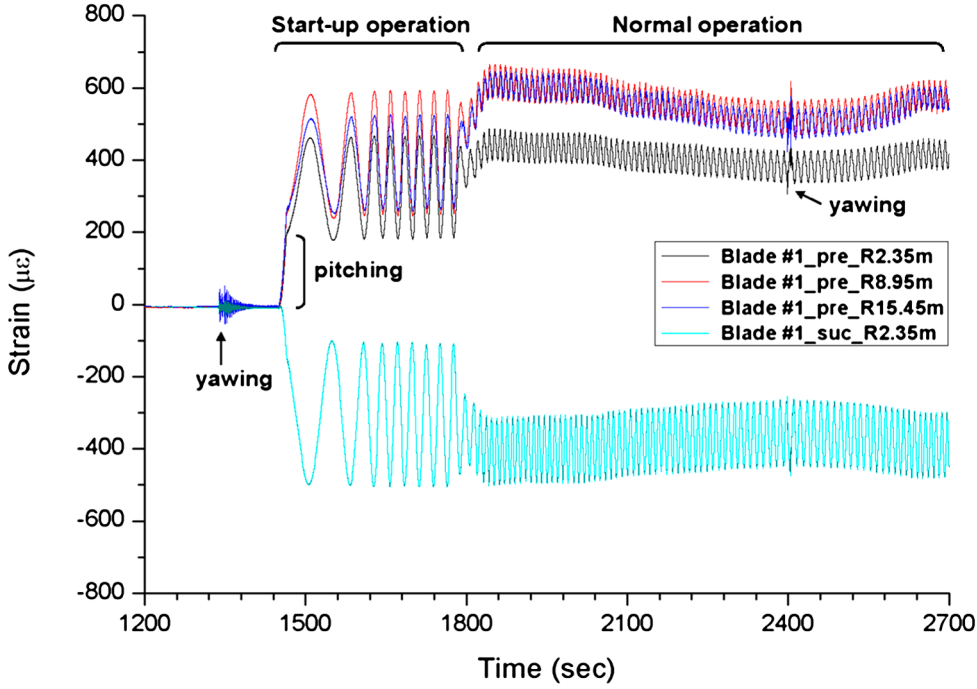

Figure 5. Test results of Blade #1. This figure is published in color on http://www.ingentaconnect.com/content/vsp/acm

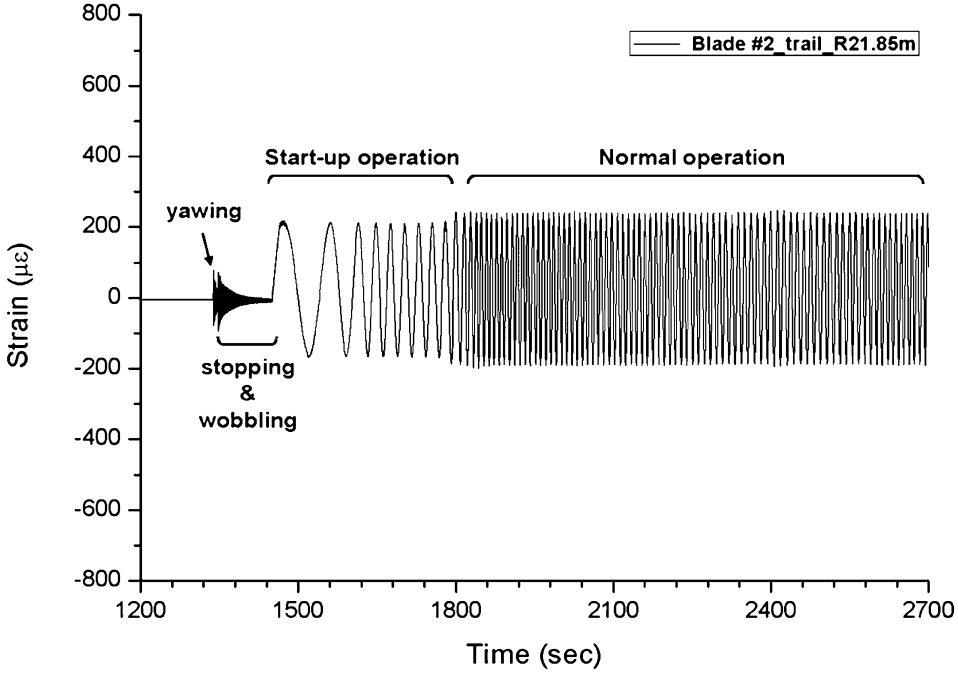

Figure 6. Test results of Blade #2.

turbine yaw system turned the rotor against the wind. After yawing stopped, the trailing edge sensor of Blade #2 more clearly indicated the wobbling of the blade, as shown in Fig. 6. A peak in normal operation of Fig. 5 was also due to changing yaw angle. Above cut-in wind speed, 3 m/s, during seconds 1450 to 1464, the pitch angle decreased from 90° to 20° at 5°/s in order to accelerate the rotation rate up to 2 rpm without generating electricity. When rotor blades accelerated to more than 2 rpm, the pitch angle decreased to 0° at 1°/s. Then the wind turbine started normal operation at 6 rpm (after 1800 s). Because of the reduced effect of blade mass by a decrease in pitch angle, pressure or suction side strain amplitude in normal operation became smaller than in start-up operation (Fig. 5). Conversely, the strain amplitude of the trailing edge became slightly larger in normal operation (Fig. 6). Overall, differences according to the operating conditions were monitored accurately in real time with FBG sensors.

3.2. Modal Analysis

Defining modal characteristics, natural frequencies and mode shapes is of paramount importance because this information can be used to avoid potentially harmful resonance behavior [7]. We have used the finite element method and the fast Fourier transform (FFT) to determine modal characteristics of rotor blades. Composite rotor blades were simulated using commercial FEM codes, I-DEAS in modeling and ABAQUS in analysis [4]. The GFRP-based rotor blade consists of an upper and a lower shell with spar caps and multi-axial sandwich shear webs as the supporting structure. The spar caps are UD (0°) glass/epoxy, the shear web is biaxial (+45°/−45°) glass/epoxy and the shells are a combination of biaxial (+45°/−45°) and triaxial (0°/+45°/−45°) glass/epoxy. Where the shell is not supported by the UD spar caps, it is built as sandwich structure with core materials such as Balsa wood and PVC foam to prevent buckling. A detailed cross-sectional view of the 2 MW rotor blade is shown in Fig. 7. Material properties of laminates used for the FE analysis are represented in Table 2. The three-dimensional finite element model has more than 200 shell element groups in the rotor blade direction and 6 element groups in the edgewise direction to apply the thickness distribution. The FE model

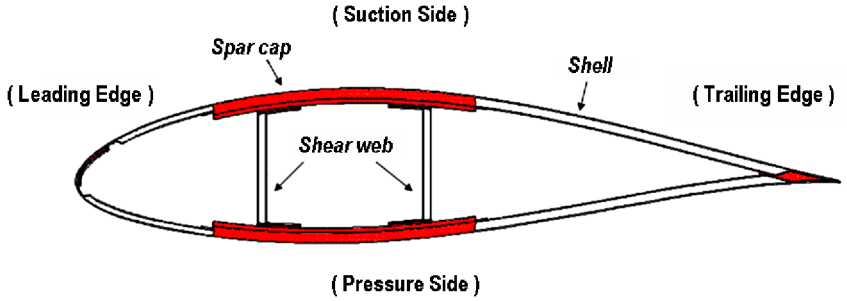

Figure 7. Cross-sectional view of the 2 MW rotor blade. This figure is published in color on http://www.ingentaconnect.com/content/vsp/acm

Table 2.
Material properties for the FE analysis

	UD (0°)	2 Ax (+45°/−45°)	3 Ax (0°/+45°/−45°)
E_1 (MPa)	41 600	11 500	29 600
E_2 (MPa)	7300	11 500	10 300
G_{12} (MPa)	4000	9700	6856
Poisson ratio	0.3	0.5	0.46
Specific weight (kg/m^3)	1880	1880	1880

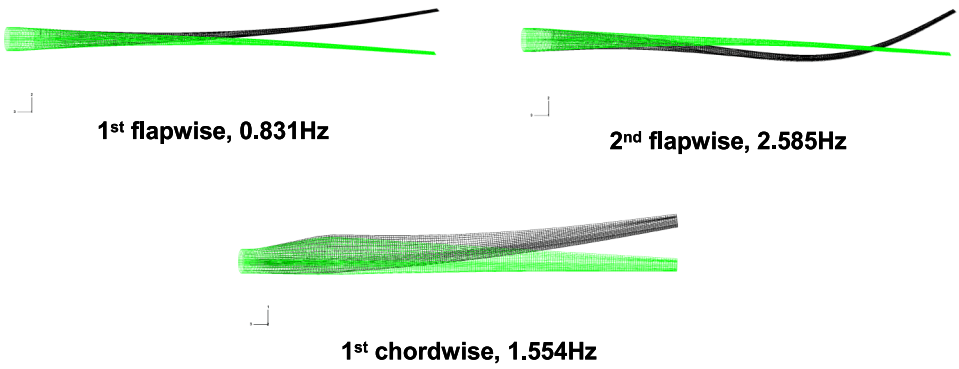

Figure 8. Mode shapes and natural frequencies from FE analysis. This figure is published in color on http://www.ingentaconnect.com/content/vsp/acm

has a 42.65 m total length and 7940 kg total weight. Figure 8 displays mode shapes and natural frequencies from FE analysis under the boundary condition of clamping the blade root.

Figure 9(b) shows the FFT result of normal operation during seconds 1900 to 2000. Main frequency, 0.105 Hz, can be converted to 6.3 rpm, which is the same as the rotational speed of the rotor blades at that moment. However, no frequencies related to natural frequencies of the blade were found, which means FBG sensors detected no excitation loadings but the effect of blade mass due to rotation (Fig. 9(a)). On the other hand, during seconds 1350 to 1450, immediately after yawing stopped, the vibration of rotor blades excited by reaction could be measured, from which the natural frequencies of the non-rotational blades were calculated (Fig. 10). The FFT result from a sensor at $R = 2.35$ m on the pressure side represents flapwise and chordwise natural frequencies compositely (Fig. 10(b)). However, a sensor at $R = 21.85$ m on the trailing edge detected only the chordwise frequency (Fig. 10(d)). In Table 3, FFT analyzed data are compared with FEM results. Except 1st chordwise, deviations for natural frequencies are within about 3%. It is considered that manufacturing error and adding balance mass to the unbalanced rotor blades caused this error.

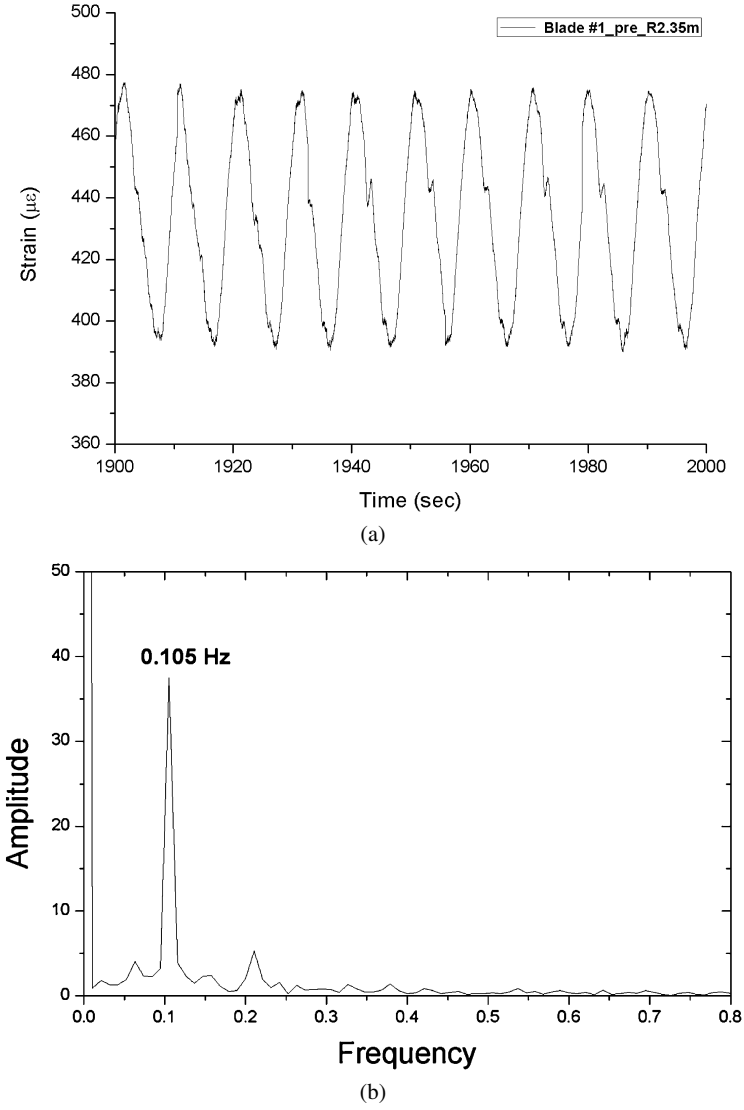

Figure 9. FFT result of normal operation at 6 rpm (1900–2000 s).

Rotation can alter the natural frequencies of certain mode shapes, when centrifugal and Coriolis forces change stiffness [7]. However, the previous calculation did not consider the effect due to centrifugal forces. Additionally, we analyzed an excited waveform at the moment of yawing during seconds 2404 to 2414 in Fig. 11(a). As a result, a noticeable frequency, 0.841 Hz, was obtained, considered as the 1st flapwise natural frequency of the rotor blade stiffened by centrifugal forces (Fig. 11(b)). This could be verified with the result that 1st flapwise natural frequency increased to 0.843 Hz from the FE analysis with centrifugal forces at 6.3 rpm.

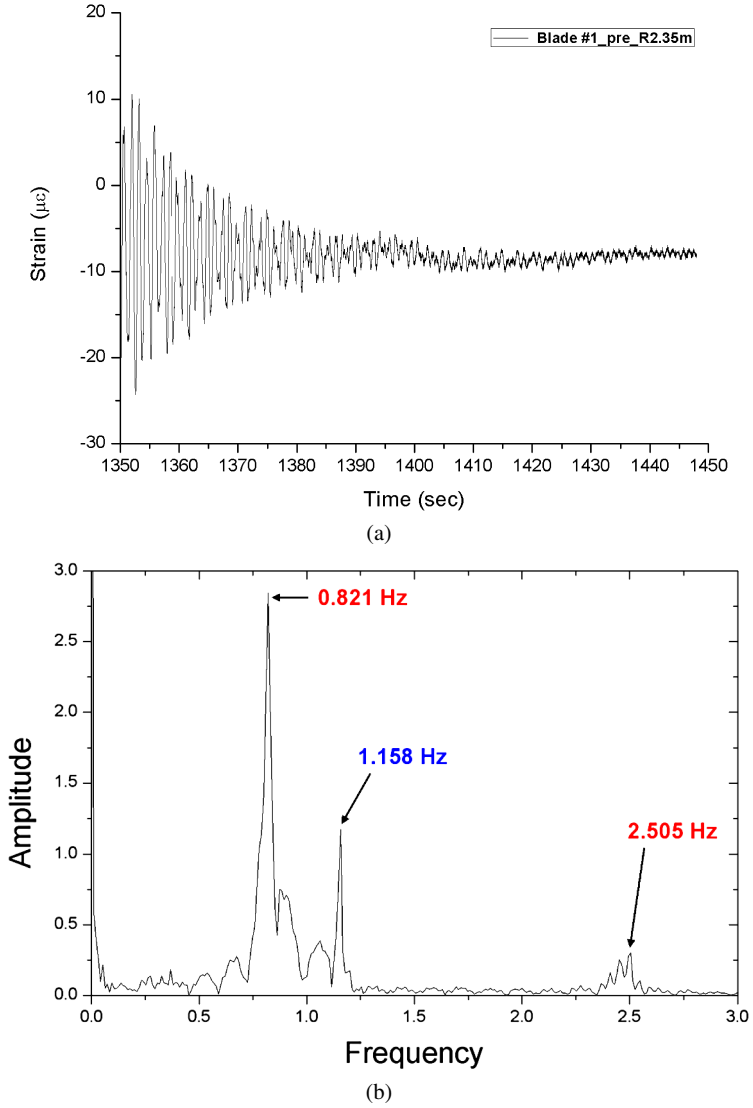

Figure 10. FFT results after yawing (1350–1450 s). This figure is published in color on http://www.ingentaconnect.com/content/vsp/acm

4. Conclusions

A real-time monitoring system with fiber Bragg grating (FBG) sensors was designed and applied successfully to monitor the operating conditions of the 2 MW wind turbine. Flapwise and chordwise natural frequencies were obtained accurately from the FFT analyzed yawing signals, and these results were compared with the FE modal analysis results of the GFRP-based composite rotor blade. Deviations of about 3% (except for the 1st chordwise natural frequency) were observed. Further-

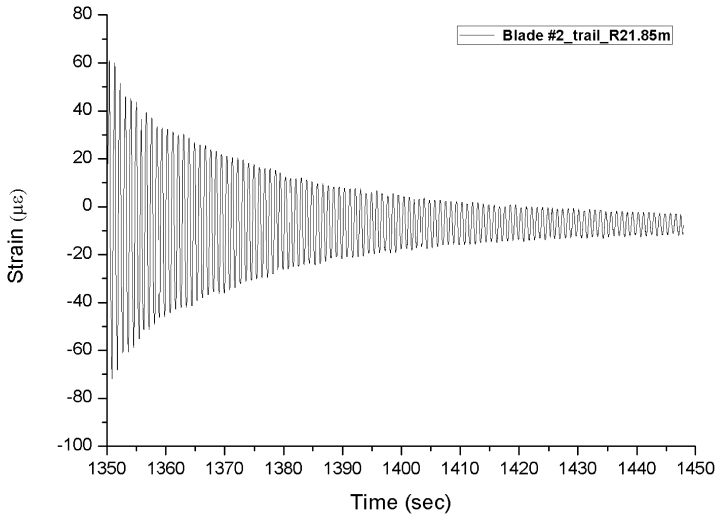

(c)

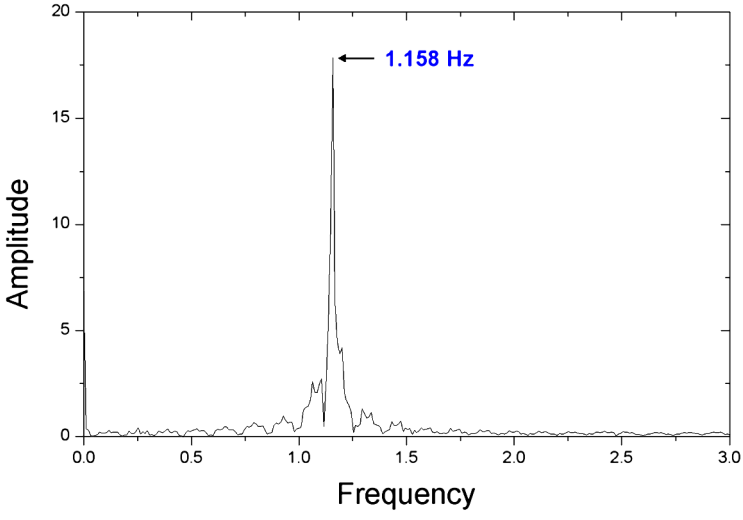

(d)

Figure 10. (Continued.)

Table 3.
Natural frequencies of the rotor blade

Natural frequency	FBG (Hz)	FEM (Hz)	Error (%)
1st flapwise	0.821	0.831	−1.2
1st chordwise	1.158	1.554	−25.5
2nd flapwise	2.505	2.585	−3.1

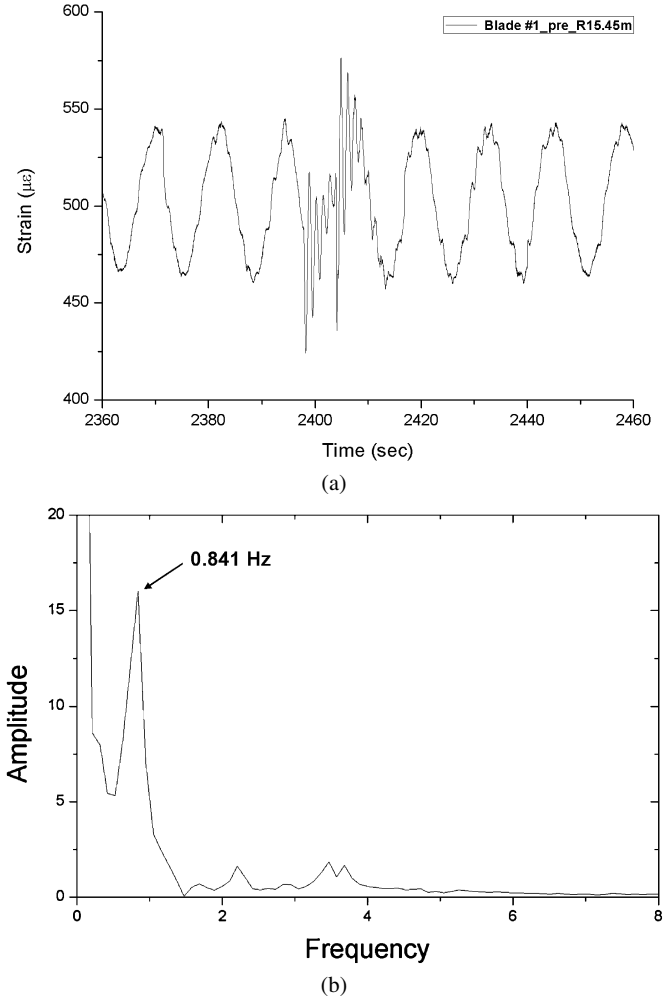

Figure 11. FFT results of normal operation at 6 rpm (2404–2414 s).

more, the system was used to monitor and verify the increase in the 1st flapwise natural frequency when the yaw angle changed, which occurs due to centrifugal forces. In the future, the capability and reliability of the applied FBG monitoring systems will be assessed. The accumulated field data will be used to understand the fatigue characteristics of rotor blades and to optimize the operating conditions of the wind turbine.

Acknowledgements

This research was financially supported by the Ministry of Knowledge Economy (MKE), Republic of Korea through the UNISON 2 MW wind turbine demonstration project.

References

1. Z. Hameed, Y. S. Hong, Y. M. Cho, S. H. Ahn and C. K. Song, Condition monitoring and fault detection of wind turbines and related algorithms: a review, *Renew. Sustain. Energy Rev*. **13**, 1–39 (2007).
2. K. Schroeder, W. Ecke, J. Apitz, E. Lembke and G. Lenschow, A fibre Bragg grating sensor system monitors operational load in a wind turbine rotor blade, *Meas. Sci. Technol*. **17**, 1167–1172 (2006).
3. L. W. M. M. Rademakers, T. W. Vebruggen, P. A. van der Werff, H. Korterink, D. Richon, P. Rey and F. Lancon, Fiber optic blade monitoring, *Paper presented at the European Wind Energy Conference* (2004).
4. S. H. Park and K. S. Han, Structural analysis and proof tests of composite rotor blades for wind turbines, in: *Proc. Intl Conf. Exhibit. Renewable Energy* (2008).
5. Free software, http://www.nqvm.com/
6. Y. J. Rao, In-fibre Bragg grating sensors, *Meas. Sci. Technol*. **8**, 355–375 (1997).
7. D. A. Spera, *Wind Turbine Technology Fundamental Concepts of Wind Turbine Engineering*. ASME Press (1994).
8. Germanischer Lloyd WindEnergie GmbH, Guideline for the Certification of Wind Turbines, Heydorn Druckerei und Berlag (2003).